TECHNICAL MEMORANDUMS

NATIONAL ADVISORY COMMITTEE FOR AERONAUTICS

No. 534

EXPERIMENTS WITH A WING MODEL FROM WHICH THE BOUNDARY IS REMOVED BY SUCTION

By Oskar Schrenk

From Luftfahrtforschung
June 11, 1928

Washington
October, 1929

NATIONAL ADVISORY COMMITTEE FOR AERONAUTICS.

TECHNICAL MEMORANDUM NO. 534.

EXPERIMENTS WITH A WING MODEL FROM WHICH THE BOUNDARY IS REMOVED BY SUCTION.*

By Oskar Schrenk.

Introduction

Under certain conditions undesirable dead regions are created in liquid and gas flows. Technically they sometimes cause very prejudicial losses of energy and other disadvantages. These losses can be avoided or reduced by drawing off small quantities of fluid from the surface into the interior of the body and thus preventing the development of turbulent regions.

The present report deals with a series of tests made for the purpose of improving flow conditions about wings by applying this suction principle (increase of the lift coefficient and reduction of the drag about very thick wing sections). Though not conclusive, the report contains interesting results.

The possibility of improving wings by removing the boundary layer by suction has frequently been considered during recent years. In this connection exhaustive tests were carried out at the aerodynamic laboratory in Göttingen. The fact that such

*"Tragflugel mit Grenzschichtabsaugung," from Luftfahrtforschung, June 11, 1928, pp. 49-62.
See also J. Ackeret, "Grenzschichtabsaugung" (Removing Boundary Layer by Suction), Zeitschrift des Vereines deutscher Ingenieure, August 28, 1926, pp. 1153-1158 (N.A.C.A. Technical Memorandum No. 395, 1927).

boundary-layer control is not yet fully satisfactory, is due to the enormous difficulties of the tests and especially to the structural problems involved. A comprehensive report of the work hitherto done seems nevertheless justified by the great interest which this problem arouses and by the results recently obtained.

The physical principle of the suction theory is simple and long since known.* On the rear side of nonstreamlined bodies, the air flow usually leaves the surface and a turbulent region without specific motion with respect to the body is formed at that point. A great thickening of the boundary layer frequently occurs without the formation of a turbulent region. The formation of these turbulent regions which, in most cases, are technically prejudicial, can be avoided frequently by drawing off small quantities of fluid from the surface (Figs. 1a and 1b). We shall not now refer to other flow phenomena which can be produced by suction.

*L. Prandtl, "Ueber Flüssigkeitsbewegung bei sehr kleiner Reibung," Verhandlungen des III. Internationalen Mathematiker-kongresses in Heidelberg, 1904 (Teubner, Leipzig, 1905). Reprinted in Vier Abhandlungen zur Hydro- und Aerodynamik, by L. Prandtl and A. Betz, Göttingen, 1927 (J. Springer, Berlin).

A. Flettner, "Anwendung der Erkentnisse der Aerodynamik zum Windantrieb von Schiffen," Zeitschrift für Flugtechnik und Motorluftschiffahrt 18, 1925, p. 53, and Jahrbuch der Schiffsbautechnischen Gesellschaft, 1924, p. 222.

J. Ackeret, "Grenzschichtabsaugung," Zeitschrift des Vereines deutscher Ingenieure, Aug. 28, 1926, p. 1153.

O. Schrenk, "Versuche an einer Kugel mit Grenzschichtabsaugung," Z.F.M. 19, 1926, p. 366.

J. Ackeret, A. Betz, and O. Schrenk, "Versuche an einem Tragflügel mit Grenzschichtabsaugung," Vorläufige Mitteilungen der A.V.A., Göttingen, No. 4, 1925.

The first technical suction tests were made by J. Ackeret and A. Betz in the Göttingen laboratory. These men likewise prompted the present tests which were made by the writer. A. Wöckner at the beginning, and B. Winkler later, participated in the tests.

II. Purpose and Development of the Tests

Boundary layer control by suction, applied to wings, insures an increase in maximum lift and permits using thick wing sections without excessive wing section or profile drag. The actual difficulty of this problem, which is simple in itself, lies in the fact that the complicated apparatus and the power required for suction must be justified from the technical point of view. Many other questions which greatly affect construction and flight, such as the space inside the wing and reliability in operation, must also be taken into consideration.

Hence the lift, drag, suction volume and suction power, the latter being chiefly the product of the suction volume by the suction pressure, had to be determined by measurement. The simultaneous, accurate and quick measurement of all these quantities caused certain difficulties. The best results were obtained up to the present time with the arrangement described in Section VIII, which consists of a model with built-in blower suspended freely from the balances in the wind tunnel. Other arrangements, in which the models were firmly secured, only permitted measuring the forces indirectly and less accurately and

quickly, owing to the connections of the suction pipes which led to the outside.

A picture of the stability of the flow produced by suction had also to be afforded by the measurements. A repetition of the tests showed certain discrepancies which did not, in general, materially affect the polar. A sensitivity to slight differences in roughness was also manifest in certain cases. Double values, analogous to those of certain wing sections in the neighborhood of maximum lift, were obtained in some cases; for example, wing sections 538-540 in Report III of the Ergebnisse der Aerodynamischen Versuchsanstalt zu Göttingen (hereafter designated as Göttingen Report I, II, or III), according to whether the point of measurement was approached from a stable form of flow (i.e., from strong suction) or from an instable one.

III. Notation

The ordinary symbols are used in the customary aerodynamic sense (ρ = air density;

v = velocity

b = span

t = chord

F = area of airfoil

A = lift

c_a = coefficient of lift

W = drag

c_w = coefficient of drag, etc.)

Compare Göttingen Report I and Fuchs-Hopf "Aerodynamik."

Q = volume of air removal per second by suction (suction volume),

$c_Q = \frac{Q}{vF}$ = nondimensional volumetric coefficient,

p = internal negative pressure in suction chamber with respect to the undisturbed external pressure,

$c_p = \frac{p}{\frac{\rho}{2} v^2}$ = nondimensional pressure coefficient,

L = total power required for flight,

$c_l = \frac{L}{\frac{\rho}{2} v^3 F}$ = corresponding efficiency ratio,

L_s = requisite suction power (See Section IV).

$c_{ls} = \frac{L_s}{\frac{\rho}{2} v^3 F}$ = corresponding nondimensional coefficient (See Section IV)

F_b = exit cross section of air flow,

$v_b = \frac{Q}{F_b}$ = discharge velocity.

IV. Evaluation of the Test Results*

In addition to lift, the total power $L = Wv + L_s$ chiefly affects the evaluation of the tests. This expression is based on the assumption of an agreement between the propeller and the blower efficiencies. The power at the crank shafts is then simply $\frac{L}{\eta}$. A difference between the two efficiencies causes a slight change in the expression $\frac{Wv}{\eta_1} + \frac{L_s}{\eta_2}$. The nondimensional form of the power equation reads $c_l = c_w + c_{ls}$. Its introduc-

*This section supplements a previous similar statement made by the writer (Z.F.M. 17, 1926, p. 366) and corrects it in one point.

tion is justified by the fact that, like the drag and lift coefficients, the boundary-layer conditions, and hence the requisite suction, are only very slightly affected by the Reynolds Number. The function of the c_a/c_w curve of normal wings is here partly assumed by the c_a/c_l curve, which, in contrast with the "c_w polar," will be called the "c_l polar."

The combination of the c_w and c_l values, as directly computed from experiments with a model is not, however, a reliable criterion of the excellence of the model, which is also affected by an arbitrarily chosen quantity, the discharge cross section F_b (Fig. 2). It appears that, whenever the flow about the model and the corresponding volumes removed by suction are given, W and L_s also depend on the discharge velocity v_b: W, because the discharge produces a certain backward thrust (i.e., a propeller effect of the blower); and L_s, owing to the blower efficiency which increases with v_b. A calculation of the minimum * shows that, in an otherwise defined case, $L = W_v + L_s$ is a minimum when $v_b = v$. Since, for a given suction volume Q, v_b depends only on F_b (See Section III), the most favorable exit section is $F_b = c_Q F$. The test results, which are given later,

*When v_b is increased by $d\,v_b$, the propeller thrust is reduced by $\rho\, Q\, d\, v_b$, and hence its efficiency is diminished by

$$d(Wv) = -\rho\, Q\, v\, d\, v_b.$$

The blower efficiency is simultaneously increased by

$$d\, L_s = Q\, d\left(\frac{\rho}{2} v_b^2\right) = \rho\, Q\, v_b\, d\, v_b.$$

The extreme minimum value of L is determined by

$$-\rho\, Q\, v\, d\, v_b + \rho\, Q\, v_b\, d\, v_b = 0$$

and lies in the neighborhood of $v_b = 0$.

are converted to this discharge section.* In this case the blower efficiency (not including resistance of pipes inside the wing) is

$$L_s = Q\left(p + \frac{\rho}{2} v^2\right)^{**}$$

where the undisturbed external pressure ($p_o = 0$) is substituted for p_o (Fig. 2) and in most cases can be accepted without hesitation. When the wing is divided into n separate suction compartments, L_s is the sum of the individual results,

$$L_s = \sum_1^n Q_i \left(p_i + \frac{\rho}{2} v^2\right)$$

just as

$$Q = \sum_1^n Q_i .$$

---

*Drag is converted as follows: the primed values being those directly obtained by experiment, the balance weighings give

$$W = W' + \rho\, Q\, v_b - \rho\, Q\, v,$$

whence, by a slight conversion, we obtain

$$c_w = c_w' + 2c_Q\left(c_Q \frac{F}{F_b'} - 1\right)$$

$$= c_w' + 2c_Q\left(\frac{F_b}{F_b'} - 1\right)$$

A cosine, originated by the direction of discharge, is thereby neglected. The conversion is superfluous for drag measurements made by the method of impulsion (See Betz, Z.F.M. 1925, p.42), since, in the most favorable case, when $v_b = v$, the impulsion effects of the intaken air and of the expelled air (Fig. 3), which are not indicated by the Pitot tube, exactly offset each other. For the sake of accuracy, the lift should also be converted in a similar manner but, in most cases, the correction is infinitely small. It was considered in only one case (Fig. 31).

**The power increment $Q \frac{\rho}{2} v^2$ represents the force of the discharge.

The following relations are thus obtained for the evaluation of the tests

$$c_Q = \sum_1^n c_{Q_i}$$

$$c_{l_s} = \sum_1^n c_{Q_i} (c_{p_i} + 1)$$

$$\therefore c_l = c_w + c_{l_s}$$

In order to proceed from an investigated case to other cases in which, for the same position on the wing, the capacity or cross-sectional area of the suction openings is different, the same flow about the wing and hence the same c_a and c_w values can be assumed as a first approximation, provided all other conditions (including c_Q) correspond. Hence, the negative suction pressure and the suction power increase with decreasing capacity of the suction openings. According to certain tests, however, (See Section V) this assumption holds true only to a limited extent. The requisite quantity seems more likely to be slightly affected by the nature of openings, perhaps due to the disturbing effects of surface conditions on the development of the boundary layer, and perhaps also to the fact that a variation in the capacity of the suction openings may affect the pressure difference required for the passage of the air and hence also the stability of the external flow about the wing.

V. Preliminary Tests with Small Models

A few preliminary tests on a small scale dealt with the question of lift increase. Owing to the small Reynolds Numbers of these tests (five to ten times smaller than those of the usual wind-tunnel tests), no data of practical value could be obtained regarding the drag reduction. The wing model (Figs. 4 and 5), of 20 cm span and 6 cm chord, was secured with its end disk to the nozzle of a small experimental blower with an opening of 200 by 200 mm (Fig. 6). For the purpose of a quick comparison with the pure potential flow about the section, one of the theoretically easily comprehensible Joukowsky sections ($f/l = 0.1$; $d/l = 0.3$)* was investigated. The lift was determined by the deflection of the jet (Fig. 6). This method is not very accurate, but very convenient for the present case.**

The most important results are shown in Figure 7. The suction volumes are plotted against the lift for two different screens (Fig. 8) located on the upper wing surface. Of the two screens tested, the slotted one is more favorable as regards the

*Regarding the J profiles, see Göttingen Report III, pages 13 and 59, and O. Schrenk, Z.F.M. 1927, pages 227 and 276.

**If β is the angle of deflection of the jet, and h the width of the jet perpendicular to the axis of the wing, then, according to the law of impulsion, we have approximately

$$c_a = 4 \frac{h}{t} \sin \frac{\beta}{2} .$$

This value must be corrected, since the deflection is not imparted to the whole volume of the jet. The air drawn off from the surface actually disappears inside the wing with about half the deflection. Hence, for a more accurate calculation, we should take $\frac{h}{t} - \frac{1}{2} c_Q$ instead of $\frac{h}{t}$.

required volume of air. Owing to its smaller capacity, however, it gives poorer results (not here indicated), especially for large c_a values. The indicated suction volumes are the minimum quantities required for the flow to conform to the surface at any angle of attack and they usually represent the most favorable test values. A further increase in suction would not materially affect the lift. A comparison with the theory of the frictionless profile flow (Fig. 9) shows a remarkable shifting of the measured lift values toward the theoretical values, according to the principles of the boundary-layer theory (Compare the relatively greater deflection of Joukowsky sections without removal of boundary layer by suction, Z.F.M., 1926, p. 225).

The c_a, α curve (Fig. 9) is derived from the test results by the following conversions: 1. The measured angle of attack is reduced by half the angle of deflection β, because the flow, on reaching the wing, has already undergone about half its deflection; 2. Along the wing, the streamlines are slightly bent, which, in the lift production, corresponds to a decrease in the effective angle of attack. A close examination shows that a bend in the streamlines $\frac{t}{r}$ (r = radius of the bend), with a reduction of $\Delta \frac{f}{t} = \frac{t}{4r}$ (f = mean camber) in the camber of the wing section, causes a reduction of $\Delta \frac{f}{t}$ in the camber and a decrease of $57.3 \times \frac{2f}{t}$ in the effective angle of attack (Compare Z.F.M., 1926, p. 225). Since, according to a vortex screen consideration, the bend in the streamlines can be expressed by

$$\frac{t}{r} = c_a \frac{t^2}{h^2} \quad 0.26$$

and hence, in the present case, by

$$\frac{t}{r} = c_a \quad 0.0234,$$

the reduction in the angle of attack, necessitated by the bend in the streamlines, is

$$\Delta \alpha^\circ = - c_a \quad 0.67^\circ .$$

Strictly speaking, in a jet of finite height h, the wing has not the same form (with respect to the flow) for different lift values. The considered wing section which, for zero lift, has a camber $f = 0.05\ t$, can, for $c_a = 6$, be identified in our arrangement with a section having a camber $f = 0.015\ t$.

An earlier test made by J. Ackeret with a very thick wing section (thickness ratio 2/3) should also be mentioned. The quantity required to produce a given lift was in this case about 40% smaller than for thinness sections. This phenomenon, which is in some way connected with the uniform pressure distribution about thick wing sections, was not, in the meantime, further investigated, since it was not originally intended to depart materially from the usual forms.

VI. Large, Internally Divided Wing Model*

The first experiments on a large scale were carried out with a wing section having a 20 cm chord like the one used for the preliminary tests (Fig. 5). The upper surface of this section consisted of the slotted screen shown in Figure 8a. The following general results were obtained.

1. The suction volume and power can be materially reduced by dividing the internal suction chamber into compartments. A correct distribution of the suction over the different steps is essential.

2. The suction volume can be further reduced by the suitable application of surface strips between the steps. Figures 11b to 11f represent various tested suction arrangements.

3. About one-tenth of the wing width at each of the free ends of the rectangular wing requires no suction since the flow there conforms automatically to the surface. Wider regions without suction cause the flow to separate along the whole wing.

The possibility of saving suction at the wing tips is due to the well-known marked decrease in lift toward the wing tips, and is also accounted for by the maximum negative pressure moving strongly backward at the tips. This prevents the separation of the flow, which can take place only in regions of increasing pressure. The width of the wing-tip region, where no suction is produced, may be slightly affected by the magnitude of the

*Short indications regarding these experiments are given in Vorlaufige Mitteilungen der Aerodynamischen Versuchsanstalt, No. 4, 1925.

lift. The width was measured for $c_a = 2.5$ (about).

Figure 12 affords an explanation of the other observations, p_a representing the direction of the external pressure about the section, which is identical in both suction arrangements. If p_i (or p_{i_1}, p_{i_2}, p_{i_3}) denotes the internal pressures in the compartments, the (hatched) pressure differences $p_i - p_a$ are then available for the passage through the grid, and it is seen that unnecessarily great suction volumes and pressures are produced under certain conditions in the rear wing region.

Contrary to former practice, the tip of a wing was placed in the air flow in the test arrangement shown in Figure 13. The other end abutted a smooth wall through which the suction was effected. This wall acted as the plane of symmetry and, except for small disturbances due to the boundary layer of the wall, this wing represented a free wing with an aspect ratio of 4. A wider wing could not be used, since greater suction volumes caused a noticeable pressure drop in the air pipes inside the wing and affected the tests unfavorably.

Among the individual results, particular attention is called to the lift measurements between $c_a = 2$ and 4* with the smallest possible suction volumes, as given in Section V. Owing to space conditions, the lift could not be measured by the former jet-deflection method and was determined in the present case by pressure-distribution measurements around the wing section,

*Local c_a values, not mean values over the whole wing span.

as made with a special pressure-testing device. For different reasons this method is not very accurate (± 10%). The most important numerical results contained in the following table were computed with corresponding values from preliminary tests.

TABLE I.

	c_a	c_Q	c_{l_s}	c_{Q_1}	c_{p_1}
Preliminary test with slotted screen	2.7	0.05			
Preliminary test with perforated screen	2.7	0.076			
Large model, suction according to Fig.11a	2.7	0.024	0.12	0.000	5.8
Large model, suction according to Fig.11b*	2.7	0.023	0.08	0.003	5.8
Large model, suction according to Fig.11c	2.7	0.016	0.05	0.002	5.8
Large model, suction according to Fig.11d	2.7	0.020	0.06	0	–
Large model, suction according to Fig.11e	2.7	0.011	0.03	0.001	4.8
Preliminary test with slotted screen	3.3	0.063			
Large model, suction according to Fig.11e	3.3	0.018	0.11	0.001	6.5

*The suction arrangements in Figures 11b to 11f were effected by pasting smooth paper over the openings.

TABLE I (Cont.)

	c_{Q_2}	c_{p_2}	c_{Q_3}	c_{p_3}
Preliminary test with slotted screen				
Preliminary test with perforated screen				
Large model, suction according to Fig.11a	0.015	6.2	0.006	1.0
Large model, suction according to Fig.11b*	0.009	4.4	0.012	2.4
Large model, suction according to Fig.11c	0.008	4.2	0.006	1.7
Large model, suction according to Fig.11d	0.005	3.7	0.015	3.0
Large model, suction according to Fig.11e	0.006	3.2	0.004	1.0
Preliminary test with slotted screen				
Large model, suction according to Fig.11e	0.014	7.5	0.003	1.2

A group of systematic tests (Fig. 14) shows the importance of a correct distribution of the suction over the individual steps. By means of these measurements, the most favorable value for $c_a = 2.7$, as indicated in Table I, was determined for the large model without uncovering. The cQ, cQ_1, cQ_2, and cQ_3 values are given in the diagram. The other values of the table likewise belong to the most favorable cases of a large series of measurements. Further tests dealt with the drag reduction of the section for lift values at which, according to Figure 10 (normal wing polar), the flow about the wing section had not yet

*See footnote, page 14.

separated (c_a in the neighborhood of 1). In principle, the suction method is also applicable when the flow behind the wing still adheres to the surface but has a greatly widened, drag-producing turbulent region. Then, however, the success will be relatively smaller than in the other case, since the flow in itself is not so unfavorable.

The tests were made by the method of impulsion (A. Betz, Z.F.M., 1926, p. 42) and gave the following results. Below $c_a = 1$, for the arrangement 11f, the reductions in power amounted to only a few per cent, while the simultaneously produced lift increments (approximately 10%) could not be accurately determined. Conditions were a little more favorable for $c_a = 1.1$. The loss curves in the wake of the wing, determined with the arrangement shown in Figure 3, are plotted in Figure 15. They show the reduction in the impulsion-loss area with increasing suction volumes and likewise the increase in lift in the form of a greater displacement of the turbulent region. The evaluation curves corresponding to Figure 15 are shown in Figure 16. They show an improvement of the total efficiency coefficient from 0.032, without suction, to 0.024 with a suction volume $c_Q = 0.0038$.

VII. Tests with Two Symmetrical Strut Sections

A case of very simple flow conditions, those of a symmetrical two-dimensional flow (zero angle of attack and side walls) about symmetrical sections of great thickness (Fig. 17), was

adopted for a thorough investigation of the profile-drag reduction and of the related problems. It was chiefly intended to throw light on the variation of the flow produced by the suction, by measuring the velocity distribution, the thickness of the boundary layer and of the turbulent region behind the wing section, as well as the pressure distribution about the wing. The testing of individual suction slots, instead of screens, was another object of the investigation.

After exhaustive tests, it was finally found impossible to undertake general flow investigations about struts. It appeared that this "symmetrical" flow is particularly unstable. The actual motion was absolutely unsymmetrical and three-dimensional and produced an irregular lift and drag distribution along the strut. Zero lift could be established only occasionally for certain wing sections. It was impossible to measure velocities and pressures in the neighborhood of the body, since the streamlines were completely changed even by a small hole or by a sounding device. An extensive incalculability range seems to be common to these struts and to the sphere in hydrodynamics. The sphere, which has been frequently used for fundamental tests in flow investigations, likewise possesses this great sensitivity to small disturbances.* Such phenomena do not surprise us when they occur about thick struts without suction, where they were observed by Prandtl many years ago. The surprising feature is

*O. Flachsbart, "Neue Untersuchungen über den Luftwiderstand an Kugeln," Physikalische Zeitschrift, 1927, p. 463.

that even the removal of the boundary layer by suction does not change these conditions. This uncertain behavior of the flow ceases, as soon as the strut is given a few degrees angle of attack. The lift and drag distribution is then much more uniform.

Numerical results could be obtained only by forming mean values along the whole strut. There is not a point where the flow separates correctly, and its drag can be affected by suction in a way similar to that of the wing in Section VI. Thick struts permit saving up to 20% of the total efficiency expressed in c_w without suction ($c_w = 0.03$ without suction). The results of a certain number of measurements with staggered struts are given in Figure 18, where l is a test value approximately proportional to the lift and representing the deflection of the wing wake from the symmetrical position as measured with the Pitot tube. $l = 10$ cm corresponds approximately to $c_a = 1$ (See Hütte I, 25th edition, p. 385).

VIII. Model with Built-In Blower - Suspension from Balance

The reliability of the results and the quick completion of the tests urgently called for force measurements with the balance. These, however, encountered great difficulties, because of the suction apparatus (Z.F.M., 1926, p. 366). These difficulties were overcome by means of a small helical blower of high revolution speed (30,000 r.p.m.), driven by one of our small three-

phase induction motors.* For the tests, as described below, the blower and the motor, together with the device for quantity measurements, were enclosed in a fuselage (Fig. 20).

Blower.- Particular attention is called to the blower with its unusually small dimensions (68 mm diameter) and great revolution speed (n = 30,000 r.p.m., peripheral velocity u = 100 m/s), which was built according to suggestions by Professor Betz. This blower was only slightly inferior to larger blowers of a similar type with the same Reynolds Number, although its practical construction as regards shape of blades, bearings and air slots between the rotor and the casing, offered greater difficulties and was perhaps less satisfactory. At 30,000 r.p.m. and for an efficiency $\eta = 0.6$, the delivery was 75 liters per second, and the pressure was 250 mm water column. The results of a special test, to which the blower was subjected, are represented in the usual way in Figure 19.** Owing to the low compression ratios (below 1.05), the thermodynamic phenomena were neglected in the evaluation of the test results. The very sensitive wood impellers, originally used, have been recently replaced by brass impellers which give excellent results and can be quickly repaired, in case of need.

Model (Figs. 20, 21a and 21b).- The wing of this model was given its unusual shape, in order that suction might permit in-

*See Göttingen Report III, p. 21, or J. Ackeret, Z.F.M., 1925, p. 44.
**See "Regeln für Leistungsversuche an Ventilatoren und Kompressoren," V.D.I.-Verlag, Berlin.

creasing the c_a value and thickening the wing section. Besides, the suction volumes and forces of this first practical model were not intended to be large. In order to achieve a thickening of the section and an increase in lift, despite moderate suction, only the central wing portion (Figs. 21a and 21b) was thickened and subjected to suction. Since the flow about the two outer wing portions without suction separated beyond a certain angle of attack, the angle of attack of these two outer portions had to be smaller than that of the central portion with suction. Subsequently, material difficulties were encountered in carrying this arrangement into effect on the first experimental airplane. Although, owing to this somewhat complicated apparatus, the accuracy of the test results was slightly impaired, they nevertheless enable general conclusions, provided certain necessary calculations are made. It was found subsequently that the irregular transition in the lift distribution produced a disproportionately high additional induced drag, which slightly impaired the test results. A more accurate evaluation of this induced drag is obtained in the following paragraph by a theoretical method.

The disks between the central and the outer wing portions serve to maintain the desired division in the lift, i.e., in the pressure distribution. They also carry the points of attachment for suspending the model. The angle of attack of the outer wing portions could be varied, owing to their mode of connection with the disks. The covers on the suction side of the central

wing portion (Fig. 20), were exchangeable and served for changing the suction openings. The static pressure was measured at three points of each suction chamber. The measuring pipes and those running from the front Pitot tubes were led to the outside at a suitable point of the lower wing surface, where they ended in small hose nozzles.

The driving motor is cooled by the air drawn off from the wing. This was the only way to keep it running for 10 minutes at full power, in spite of its necessarily very small size. Owing to the rapid vibrations (up to 500 per second), model parts in direct connection with the motor and/the blower wore out rapidly and some of them had to be replaced during the tests.

Principal dimensions of the model:

Wing chord, uniform	200 mm
Wing span, over-all	1200 "
Span of central wing portion	450 "
Thickness of central wing portion	68 "
Thickness of outer wing portions	30 "
Height of disks	140 "

Induced drag of model.- As previously stated, the angle of attack and hence the lift c_a of the central wing portion must be larger than those of the outer wing portions. The resulting lift distribution is shown in Figures 22a and 22b. As a first approximation, the c_a difference between the central and the outer wing portions are considered constant for a certain differ-

ence $\Delta\alpha$ between the angles of attack of the two portions. After several tests, $\Delta\alpha = 5^{\circ}$ was adopted. This corresponds to a difference of 10 to 15° in the axes of zero lift and of perhaps $\Delta c_a = 0.8$ to 1.0 in the lift.

According to the wing theory, such a distribution permits the anticipation of an induced drag greater than the theoretical minimum, which is shown to be developed by an ordinary wing without disks, when the lift distribution is elliptic. According to previous experiments, no material departure from the theoretical minimum was originally assumed. Owing to the unusual drag distribution, however, this additional induced drag was found, during the tests , to exceed materially the assumed value. Thus, in the original results, these induced drag increments were more manifest than the favorable suction effect.

Nevertheless, in order to enable conclusions regarding this suction effect, the profile drag of the model had to be plotted subsequently as the difference between the total and the induced drags. The relation between the profile drag and the suction strength is thus generalized, since it becomes independent of the particular form of the model.

In order to determine the model profile drag by the specified method, the following course was followed, which led approximately to the goal. The wing was considered as a biplane structure with two geometrically similar wings of unequal span. Furthermore, an elliptic lift distribution was assumed over the

longer of these two wings (with full span of model), while, over the shorter one, it corresponded to that of a wing with end disks of the above-given dimensions. The actual lift of the model could be obtained by the superposition of the two lift distributions. Let the subindex 1 denote the values belonging to the longer wing and the subindex 2 denote the values belonging to the other wing. Then c_a and c_w refer to the corresponding areas $b_1 t$ and $b_2 t$. The induced drag for this arrangement is defined by the general equation

$$W = \int d W = \int \frac{\omega}{v} d A,$$

ω being the downward velocity produced by the wing. In the case under consideration the equation is resolved into the following members:

$$W = \int \frac{\omega_1}{v} d A_1 + \int \frac{\omega_2}{v} d A_2 + \int \frac{\omega_1}{v} d A_2 + \int \frac{\omega_2}{v} d A_1 =$$

$$= W_{11} + W_{22} + 2 A_2 \frac{\omega_1}{v},$$

where W_{11} is the first integral or the drag of wing 1, and W_{22} the corresponding integral of wing 2. The third and the fourth integrals denote the mutual interferences which are equal, according to an equation originally indicated by Munk ("Dissertation," Göttingen, 1919). They can be summed up by $2 A_2 \frac{\omega_1}{v}$, since $\frac{\omega_1}{v}$ is constant.

The correspondingly reduced expression reads

$$c_w = c_{w_{11}} + c_{w_{22}} \frac{b_2}{b_1} + 2\, c_{a_2} \frac{b_2}{b_1}\, c_{a_1} \frac{t}{\pi b_1}$$

$$= \frac{t}{\pi b_1} \left\{ c_{a_1}{}^2 + \kappa\, c_{a_2}{}^2 + 2\, c_{a_1}\, c_{a_2}\, \frac{b_2}{b_1} \right\}.$$

κ is the applicable factor of the induced drag (See Göttingen Report III, p. 17) of the wing with the disks in question. In the present case $\kappa = 0.64$. The minimum induced drag for the same mean

$$\bar{c}_a = c_{a_1} + \frac{b_2}{b_1}\, c_{a_2}$$

of the wing without disks (elliptic lift distribution) is calculated in the usual way for comparison.

$$\bar{c}_w = \frac{\bar{c}_a{}^2\, t}{\pi\, b_1} = \frac{t}{\pi\, b_1} \left\{ c_{a_1}{}^2 + 2\, \frac{b_2}{b_1}\, c_{a_1}\, c_{a_2} + \frac{b_2{}^2}{b_1{}^2}\, c_{a_2}{}^2 \right\}.$$

The difference between the two drags is:

$$c_w - \bar{c}_w = \frac{t}{\pi b_1} \left\{ \kappa - \frac{b_2{}^2}{b_1{}^2} \right\} c_{a_2}{}^2 .$$

In the approximation represented by this calculation, the difference, with respect to the minimum induced drag, is seen to be independent of $\bar{c}_a$. Then c_{a_2} is considered as a pure function of $\Delta\alpha$, whence a drag parabola, shifted about $c_w - \bar{c}_w$ to the right, is obtained in polar representation for a specific model.

In the present case, the polar is subjected to a parallel displacement of $\Delta c_w = 0.026$ for $c_{a_2} = 1.0$ and $\Delta\alpha = 5^\circ$, and of $\Delta c_w = 0.017$ for $c_{a_2} = 0.8$. A careful evaluation

shows that the profile coefficients of glide are materially improved by subtracting this additional induced drag. In order to emphasize this fact, the parabola with $\Delta c_w = 0.02$ is plotted as a dot-and-dash line in the following diagrams, in addition to the parabola of minimum drag. After the subtraction of these two drag portions, the profile drag remains between the dot-and-dash parabola and the test curve.

Tests and results.- Aside from the above-mentioned difficulties, which were due to material stresses, the progress of the measurements was much easier than before and a larger number of results was obtained. The method adopted for the completion of the tests consisted in first measuring the forces (drag and lift) simultaneously from a group of points by means of the wind-tunnel balances and then, after fitting the necessary pipes, determining, in the air flow, the pressures and quantities by means of a photographic multiple manometer. Identical flow conditions, for each two corresponding individual measurements, were insured by accurate observation with a sounding wire.

Thus, in the course of extensive experimentation, there were investigated different strengths of suction, different suction-load distributions over the two chambers and especially suction openings of different size, position, number and shape. It may already have been noted that the form of the suction slots (sharp-edged or rounded-off) was quite negligible. Disregarding the unfavorable aspect ratio and the great suction force, great lift

values for the central wing portion alone (Figs. 31 to 33) were finally investigated.

In the representation of the results, the c_a, c_w, and c_l values, obtained with specific arrangements of the suction openings, are plotted on each pair of diagrams and the corresponding suction coefficients are indicated in numerical tables. The individual curves are lines connecting points of approximately equal suction strength. The figures in the numerical tables are mean values from the measurements for each point ($\pm$ 5%). As regards the reduced values c_a, c_Q, etc., a decrease in the airstream velocity roughly corresponded to an increase in the number of revolutions of the blower. This fact was taken advantage of in cases of strong suction when the blower was inadequate. There nevertheless remained the usual slight uncertainty regarding the influence of the different Reynolds Numbers.

Only the most important results of a large series of tests are given in Figures 24 to 30. The unpublished results are nearly as satisfactory, however, in all essential respects. The compilation of the results shows a characteristic behavior of the c_l polars. With increasing angle of attack, the most favorable $\frac{c_l}{c_a}$ values follow gradually increasing suction volumes. The combination of the most favorable values of a diagram produces an envelope polar which seems to be the best criterion for the excellence of the arrangement. The comparable envelope polars are shown separately in Figure 30.

The c_w polars chiefly afford a definite idea of the flow about the model, while the frequent coincidence of curves with different suction strengths proves that the flow often fails to be further improved after it has been brought to conform to a surface. Where curves with different suction strengths coincide, it shows that the flow undergoes no material changes when the suction is increased beyond a certain limit.

Cases of identical suction arrangements but of different step loadings (different positions of the throttle valve) are not indicated in the results, since even quite large changes in the distribution of c_{Q_1} and c_{Q_2} or of c_{p_1} and c_{p_2} (up to 100%) do not produce substantial differences in the c_l polars, provided the c_{l_s} values approximately agree. According to the numerical tables for Figures 26 and 27, good flow conditions are also produced by equal pressure in both chambers. Hence, contrary to former observations, this model does not require compartments. The results hitherto obtained do not definitely settle the question of when to use compartments.

Summary

The improvement of wings is directly affected by the described tests. Indirectly, they are of interest in cases when liquid or gas flows can be technically improved by preventing turbulent regions.

According to the results, wings hitherto considered unfit

for use in airplane construction, owing to their thickness and angle of attack, were so far improved by suction as to become technically usable. Owing to the many possibilities of applying suction methods in airplane construction, no final idea of the attainable results can yet be afforded by the tests. Close cooperation of the designer and of the aerodynamic expert is perhaps the best and shortest way to reach a solution.

Beyond $c_a = 1$, sections with a thickness ratio of approximately 1 : 3 can be materially improved (up to 30%). Thus, from the aerodynamic viewpoint, very thick sections, which are sometimes statically desirable, are only slightly inferior to those used at the present time. Profile-drag coefficients of $c_w = 0.03$ and upward can generally be much improved, whereas more favorable original conditions cannot be. For the model described in Section VIII, with a central wing portion from the surface of which air is removed by suction (Fig. 21), profile coefficients of glide of approximately 1/40 to 1/50 are obtained after deduction of the rather great induced drags (Section VIII, 2). Moreover, the model in itself is not particularly favorable as regards profile drag (friction and possible separation drag due to the end disks).

As regards the lift, c_a values up to 6 ($c_Q = 0.2$) were reached in one case (Section V) and up to $c_a = 4$ ($c_Q = 0.05$) in another case (Section VIII) by the application of great suction strengths. Lift values up to $c_a = 2.0$ were also measured for

the complete model in Section VIII (Fig. 21). They had considerable profile drag, owing to the fact that the flow about the outer wing portions was already half-detached (Figs. 24 to 29).

Technically speaking, the data of Section VII deserve consideration. They prove that all accurate methods of measurement fail when applied to nonlifting flow about symmetrical thick sections. This fact is accounted for by the formerly often-observed instability of such flows which could not be prevented by suction. The good agreement between the lift of the calculated potential flow and that of the actual flow produced by suction (Fig. 9, Section V) is in harmony with theoretical considerations.

Lastly, it should be noted that the Reynolds Number of the described test is exceeded by that of actual airplanes at least by a factor of 10. Although experience shows that the forces acting on a model are approximately proportional to those exerted on full-size airplanes, it is doubtful whether these conditions also hold good for suction volumes, since the boundary-layer theory suggests the idea of a gradual decrease in the suction volume with increasing Reynolds Number. However, for lack of practical experience, no definite statements can be made.

TABLE II. (Fig. 24)

	c_Q	c_p	c_{l_s}
a	0.0005	0.7	0.0008
b	0.0010	1.5	0.003
c	0.0020	2.8	0.008
d	0.0031	3.7	0.014
e	0.0046	5.3	0.030
f	0.0075	8.9	0.074

TABLE III (Fig. 25)

	c_Q	c_p	c_{l_s}
a	0.0005	0.4	–
b	0.0019	0.8	0.003
c	0.0032	1.5	0.008
d	0.0044	2.7	0.016
e	0.0059	4.6	0.033
f	0.0089	8.5	0.085

TABLE IV (Fig. 26)

	c_{Q_1}	c_{Q_2}	c_Q	c_{p_1}	c_{p_2}	$c_{l_{s_1}}$	$c_{l_{s_2}}$	c_{l_s}
a	–	–	–	–	–	–	–	–
b	–	0.0016	0.0016	1.5	1.3	–	0.004	0.004
c	0.0006	0.0027	0.0033	2.2	2.1	0.002	0.008	0.010
d	0.0007	0.0040	0.0047	2.8	2.8	0.003	0.015	0.018
e	0.0012	0.0056	0.0068	3.5	3.6	0.005	0.026	0.031
f	0.0034	0.0071	0.0105	5.3	5.9	0.021	0.049	0.070

TABLE V (Fig. 27)

	c_{Q_1}	c_{Q_2}	c_Q	c_{p_1}	c_{p_2}	$c_{l_{s_1}}$	$c_{l_{s_2}}$	c_{l_s}
a	–	–	–	0.6	0.5	–	–	–
b	–	0.0012	0.0011	1.3	1.3	–	0.003	0.003
c	0.0005	0.0019	0.0024	2.5	2.3	0.002	0.006	0.008
d	0.0013	0.0022	0.0035	3.3	3.1	0.006	0.009	0.015
e	0.0075	0.0030	0.0056	4.7	4.1	0.014	0.015	0.029
f	0.0043	0.0044	0.0086	6.8	6.6	0.033	0.034	0.067

TABLE VI (Fig. 28)

	c_Q	c_p	c_{l_s}
c	0.0031	1.4	0.007
d	0.0040	1.6	0.010
e	0.0055	2.7	0.021
f	0.0088	5.7	0.058

TABLE VII (Fig. 29)

	c_{Q_1}	c_{Q_2}	c_Q	c_{p_1}	c_{p_2}	$c_{l_{s1}}$	$c_{l_{s2}}$	c_{l_s}
c	–	–	0.0035	1.6	1.3	–	–	0.007
d	0.0004	0.0040	0.0048	2.0	1.6	0.001	0.011	0.012
e	0.0020	0.0048	0.0068	2.8	2.5	0.007	0.017	0.023
f	0.0045	0.0055	0.0100	3.9	3.8	0.021	0.028	0.048

TABLE VIII (Fig. 30)

	c_{Q_1}	c_{Q_2}	c_Q	c_{p_1}	c_{p_2}	$c_{l_{s1}}$	$c_{l_{s2}}$	c_{l_s}
a	–	0.010	0.010	3.3	2.6	–	0.036	0.036
b	0.003	0.010	0.016	4.2	3.7	0.026	0.047	0.073
c	0.010	0.016	0.026	5.9	5.6	0.068	0.105	0.170
d	0.023	0.027	0.050	12.0	11.9	0.290	0.330	0.630

Translation by W. L. Koporindé,
Paris Office,
National Advisory Committee
for Aeronautics.

Fig.1a Flow about a wing without removal of boundary layer by suction(with turbulent region.)

Fig.1b Flow with removal of boundary layer (no turbulent region.)

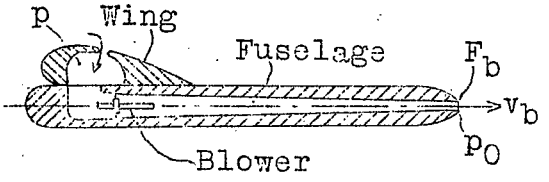

Fig.2 Diagrammatic section of air passing through a model or an airplane with suction.

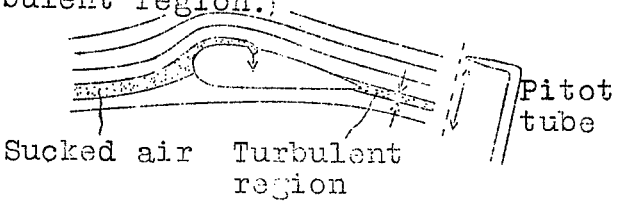

Fig.3 Drag measurement of a suction wing by impulsion method.The outlet for the sucked air is not supposed to lie in the cross-sectional plane in which the measurement is made.

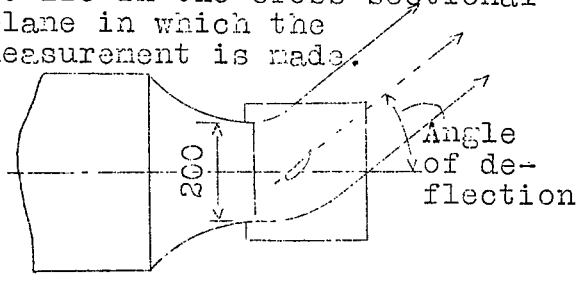

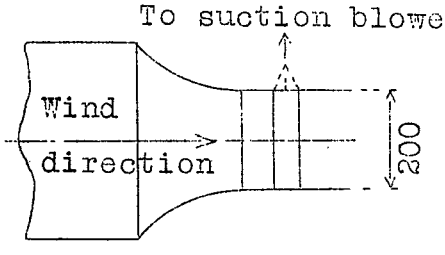

Fig.6 Arrangement for the tests in Section V.

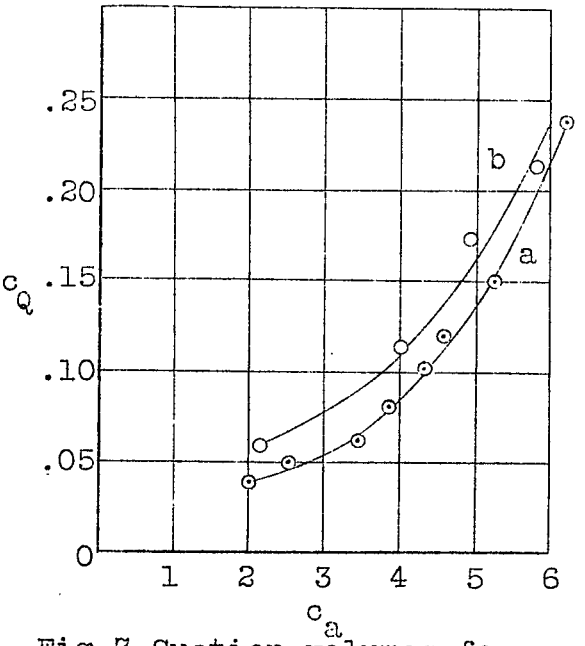

Fig.7 Suction volumes for c_a values 2 to 6,measured with model in Fig.4Curve a was obtained with slotted screen (Fig.8a)and curve b with perforated screen(Fig.8b)

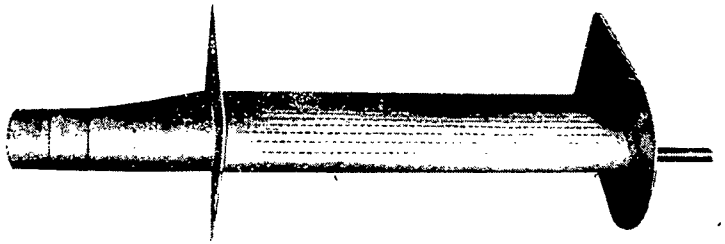

Fig.4 Test model for the preliminary tests. (Section V)

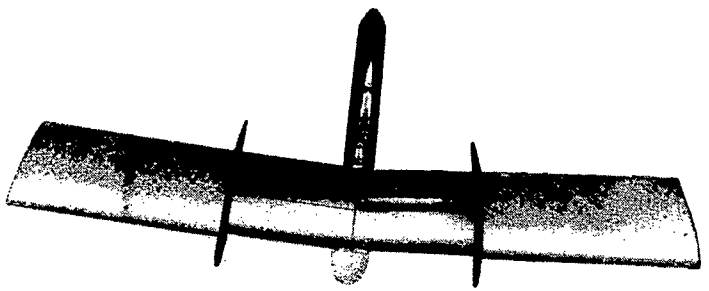

Abb. 21a.

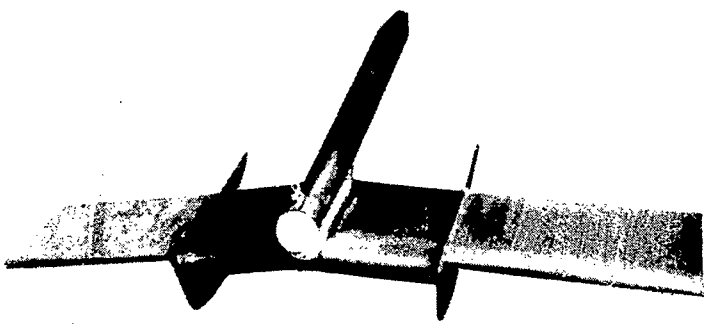

Figs.21a & 21b Model in Section VIII.

Figs. 32 & 33

Flow conditions according to Fig.31, with & without suction. Suspension of model in front of cone of small wind tunnel, shown in the two figures, was intended only for photographic purposes

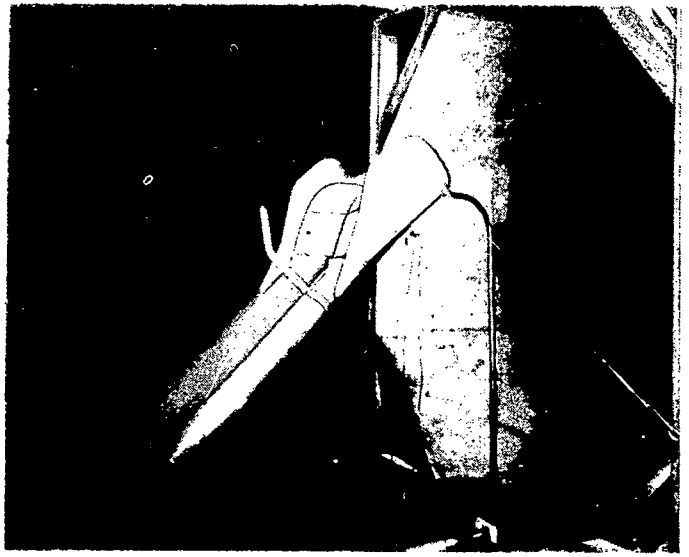

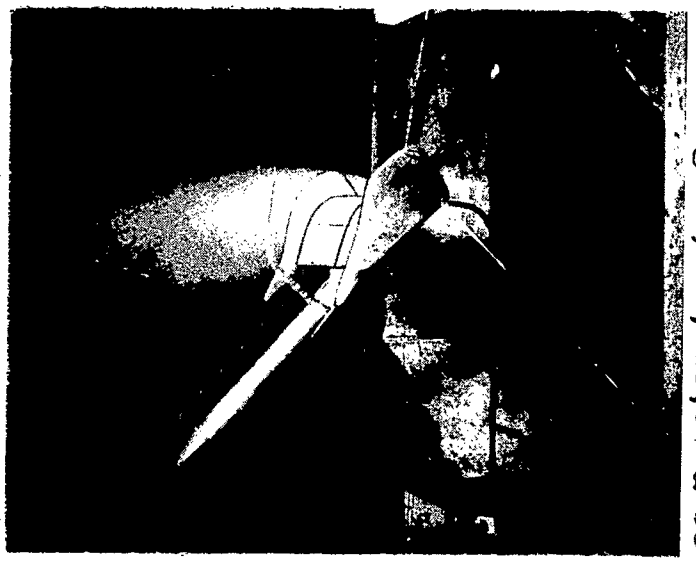

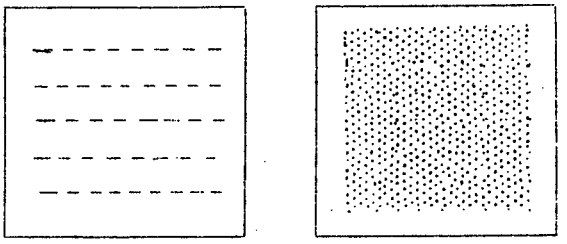

Fig.8a Fig.8b

Fig.8 Suction screens.(a)Slotted screen,air removed 0.75m^3/sec/m^2at 1mm water.(b)Perforated screen,under same conditions air removed is 0.5m^3/sec.Slotted screen was used for models in Section V and VI (flow perpendicular to direction of slots), perforated screen for models in Sections IV and VII.

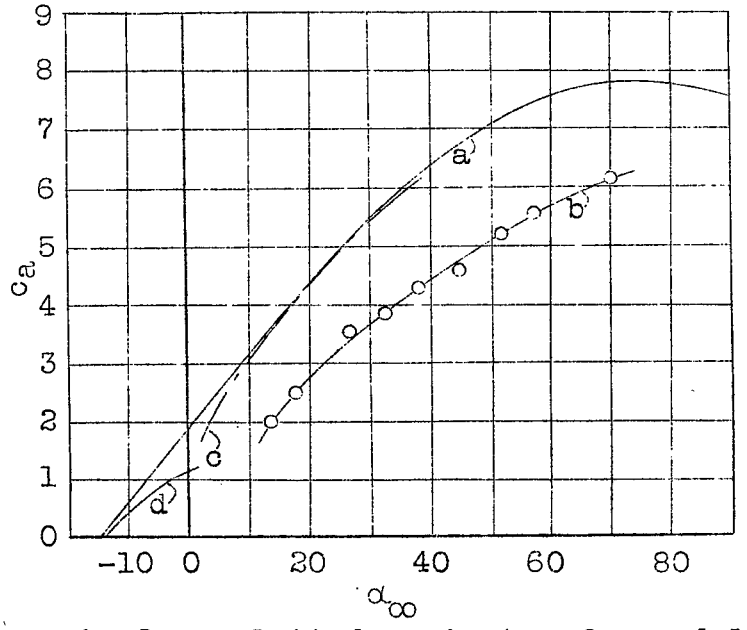

Fig.9 c_a plotted against α for model in Fig.4.(a) Theoretical frictionless flow,(b) Measured values of suction wing.(c)Same values converted to infinite height of jet h. (d) Measurements on normal wing (20 $\times$ 100cm^2) without suction,converted to infinite aspect ratio.(See Fig.10)

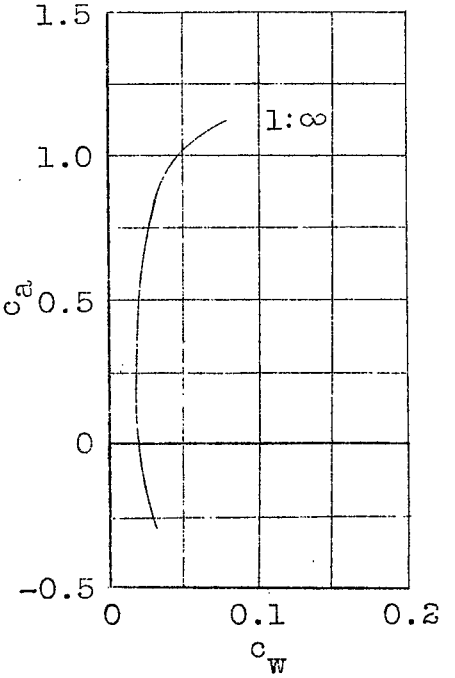

Fig.10 Polar of Joukowsky section. f/l=.1,d/l=.3 as normal wing converted to infinite aspect ratio.

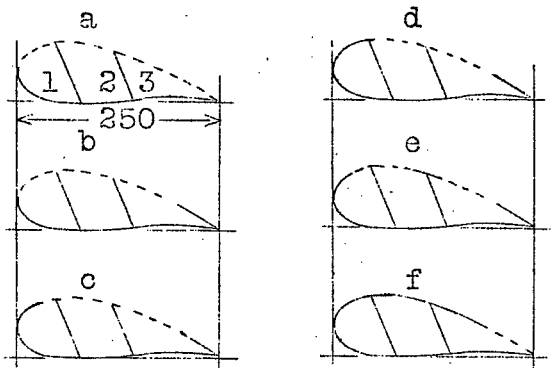

Fig.11 Wing profiles in Section VI, same as in Fig.5, wing compartments and different locations of suction regions.

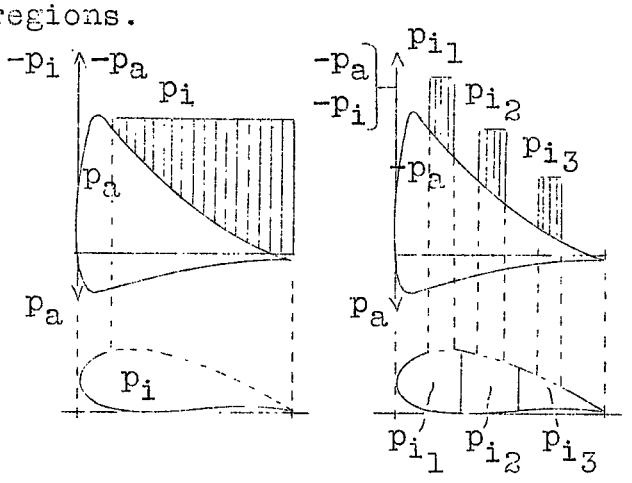

Fig.12 Effect of covering and of wing compartments on suction volumes and forces.

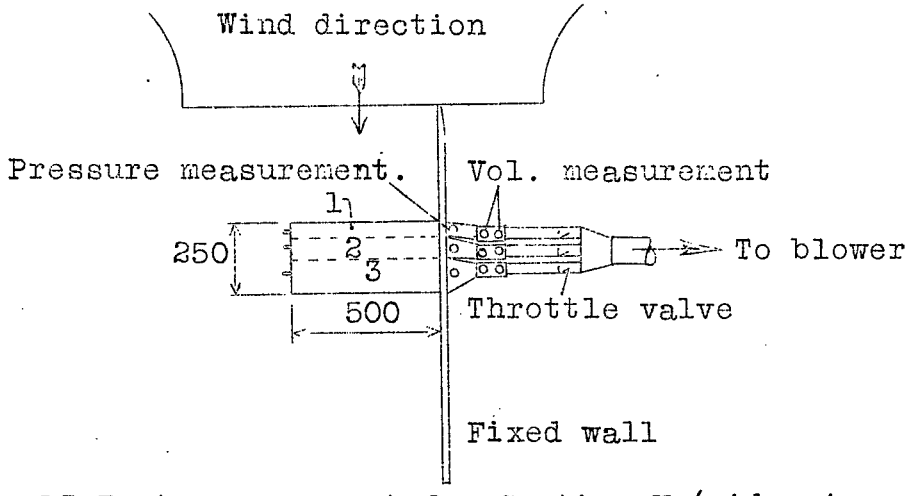

Fig.13 Test arrangement for Section V (side view similar to Fig.6).

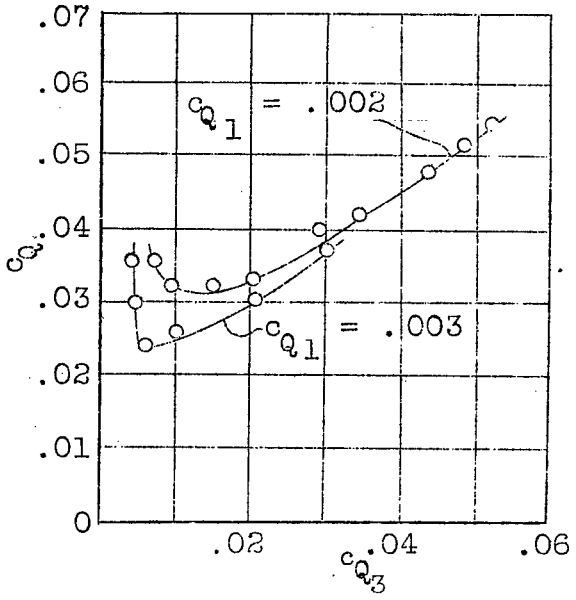

Fig.14 Experimental determination of favorable load distribution over 3 suction steps. For c_a=2.7 the curves correspond to Fig.11a (See Table I) c_{Q_1} is constant for each curve, c_{Q_3} and c_Q can be estimated ($c_{Q_2}=c_Q-c_{Q_1}-c_{Q_3}$).

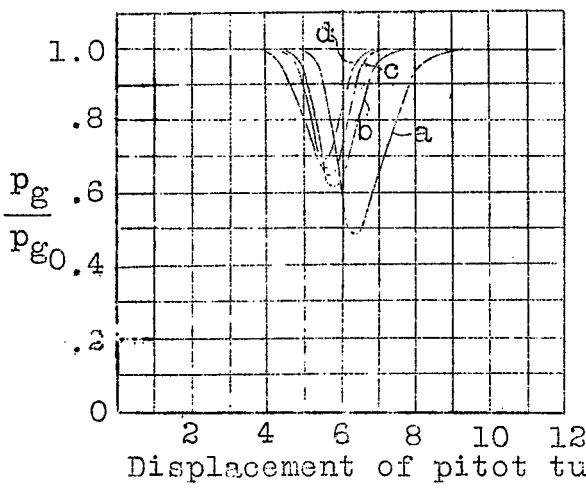

Fig.15 Curves of loss of impulsion behind wing, for determining drag. Loss of impulsion per unit time is simply replaced by loss in total pressure p_g, allowance being made for small errors. For a), c_Q=0, for b), c_Q=.0038, for c), c_Q=.0070, for d), c_Q=.0097, (See ZFM, 1925, p.42).

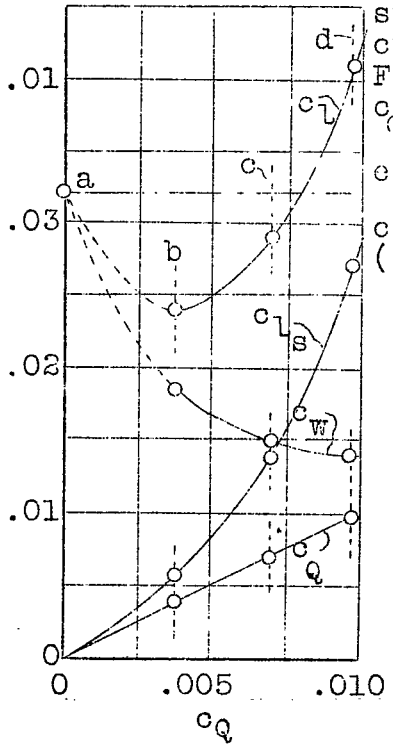

Fig.16 Evaluation curves for Fig.15. Dot and dash line denotes drag without suction.

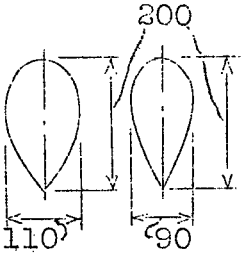

Fig.17 Strut sections from Section VII. Suction slots occupied various points in central third of chord.

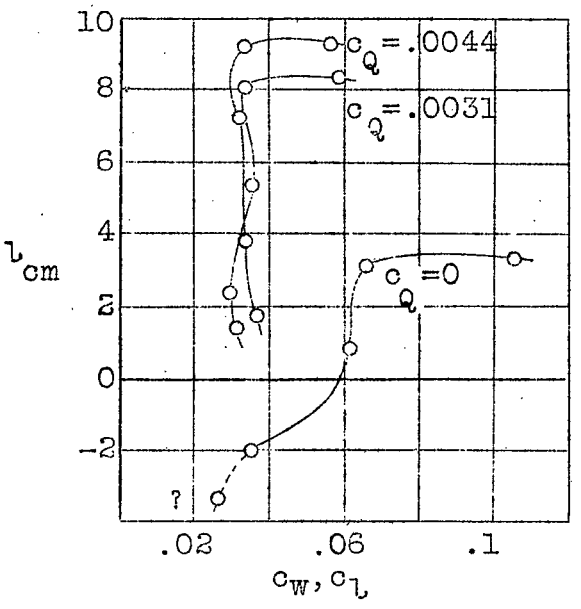

Fig.18 Polar of thick strut with different suction strengths. l is proportional to c_a. l=10cm about. c_a=1

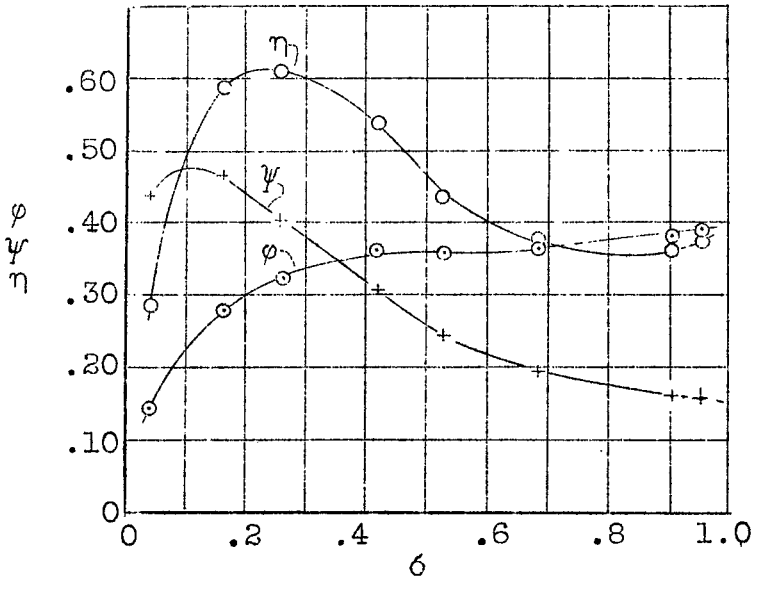

Fig.19 Characteristic curves of small experimental blower in Section VIII. Notation. $u=\omega r$=peripheral velocity of impellers; p=difference between static pressure forward and aft of blower; v=velocity of flow through the annular section swept by impeller blades. $\varphi=v/u$=delivery coefficient; $\psi=p \div \rho/2u^2$=pressure coefficient; η=efficiency, $\sigma = \frac{\frac{\rho}{2} v^2}{d+\frac{\rho}{2} v^2}$ represents throttle condition at which blower works.

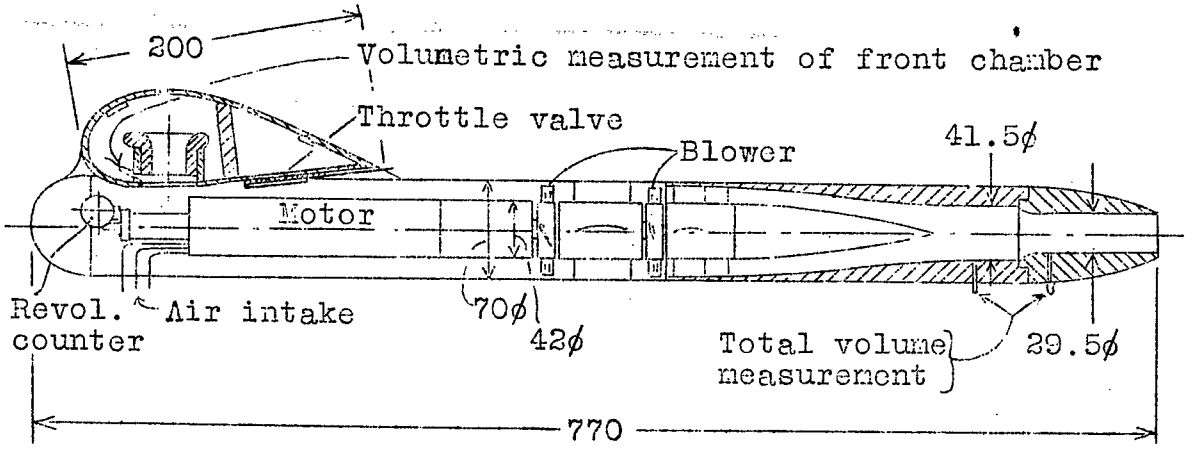

Fig.20 Central cross section through model in Section VIII.

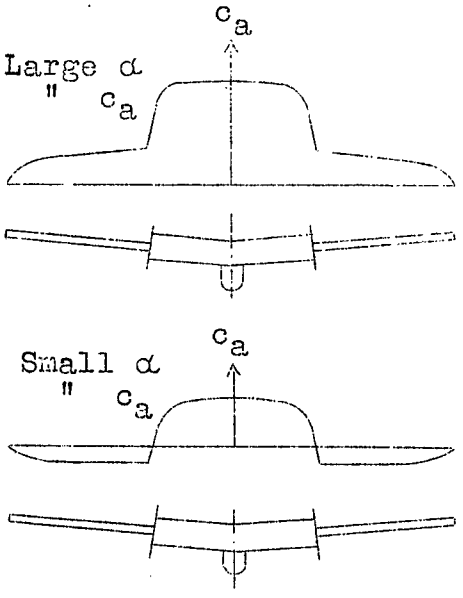

Fig.22a & 22b Approximate lift distributions about model in Figs.21a & 21b.

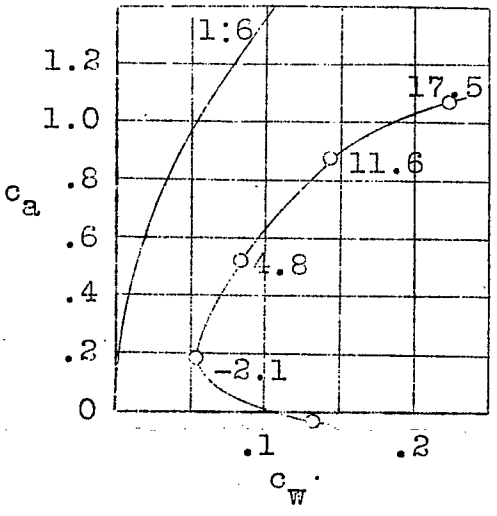

Fig.23 Polar of model in Section VIII, without suction.

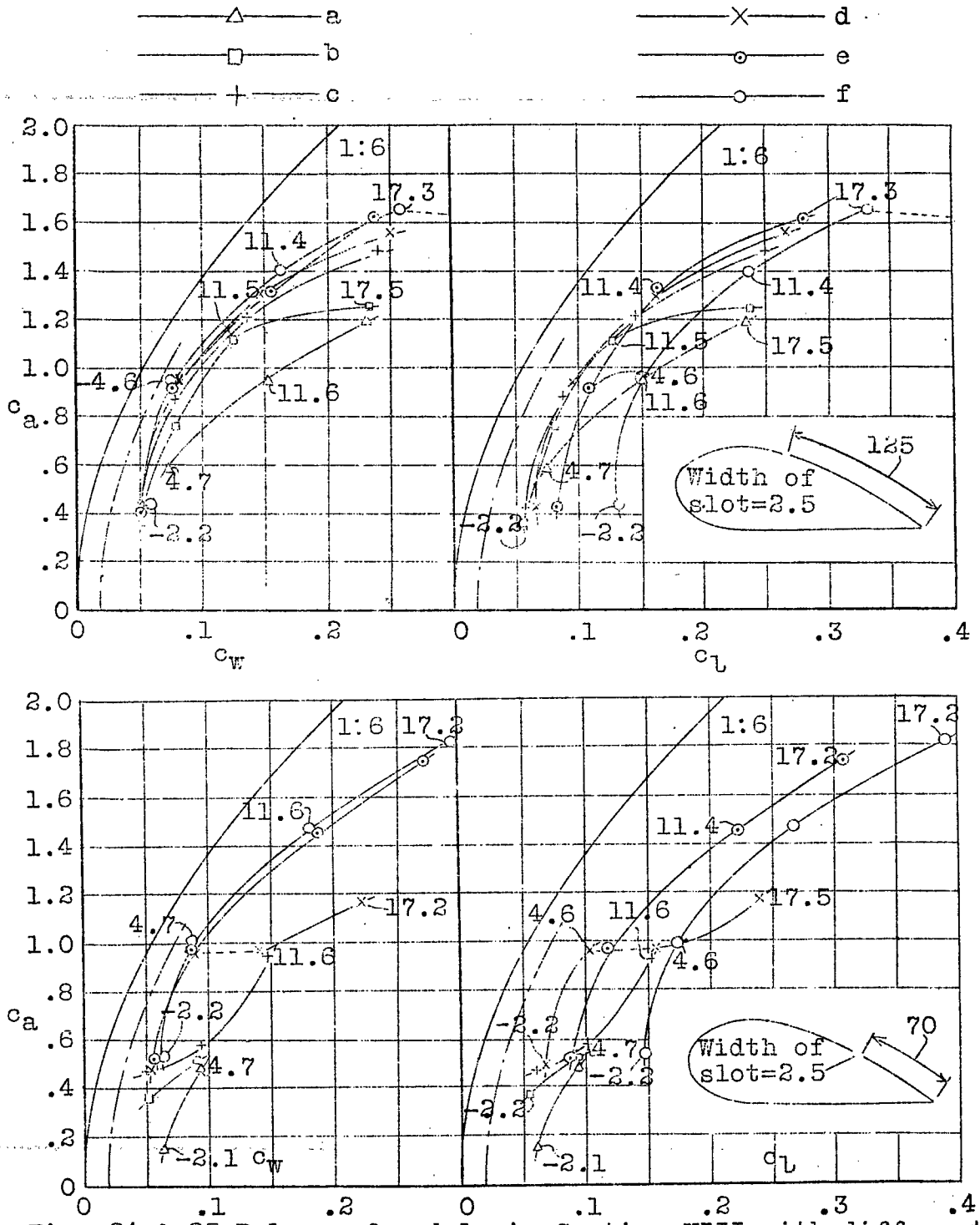

Figs.24 & 25 Polars of models in Section VIII with different suction arrangements.

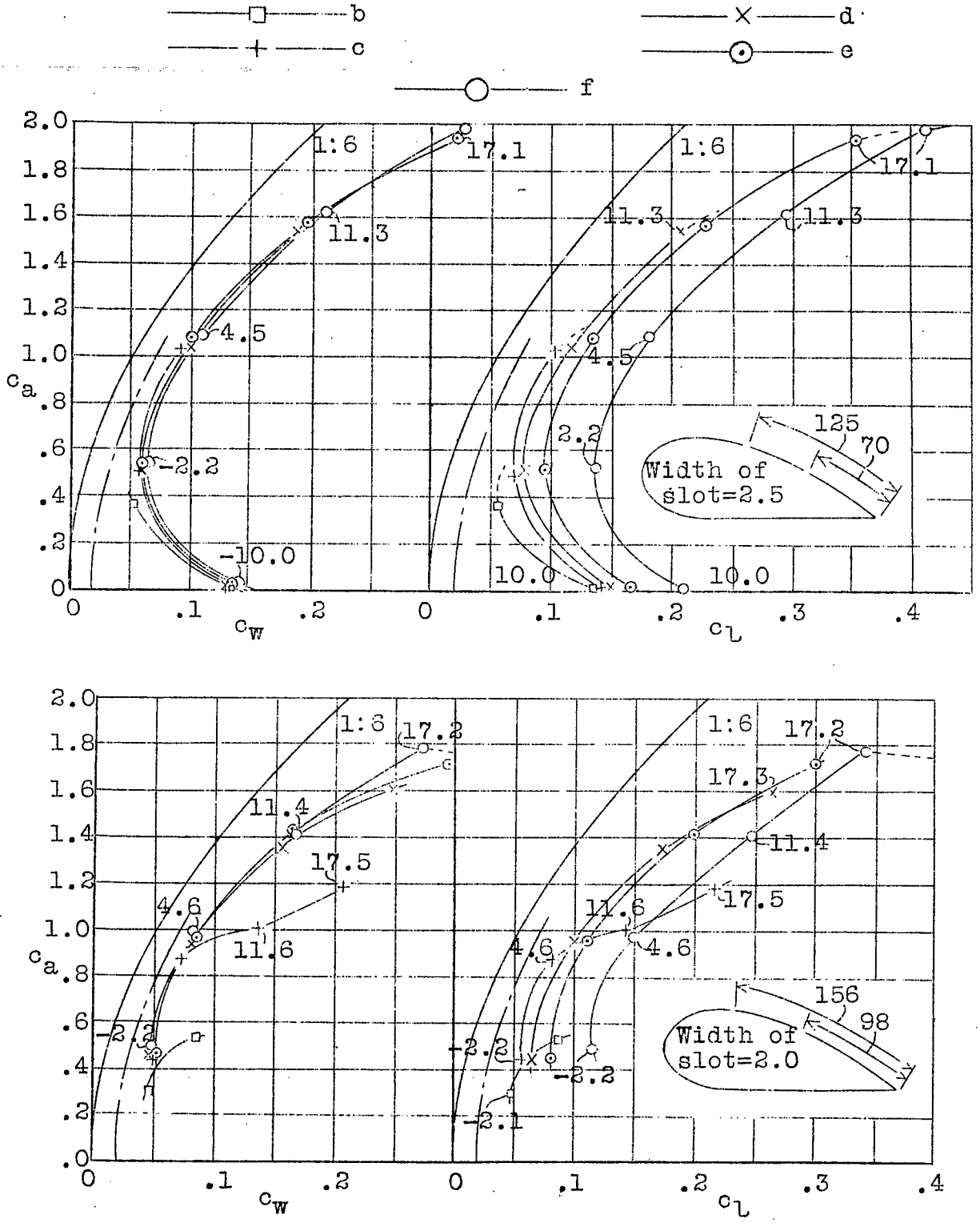

Figs.26 & 27 Polars of models in Section VIII with different suction arrangements.

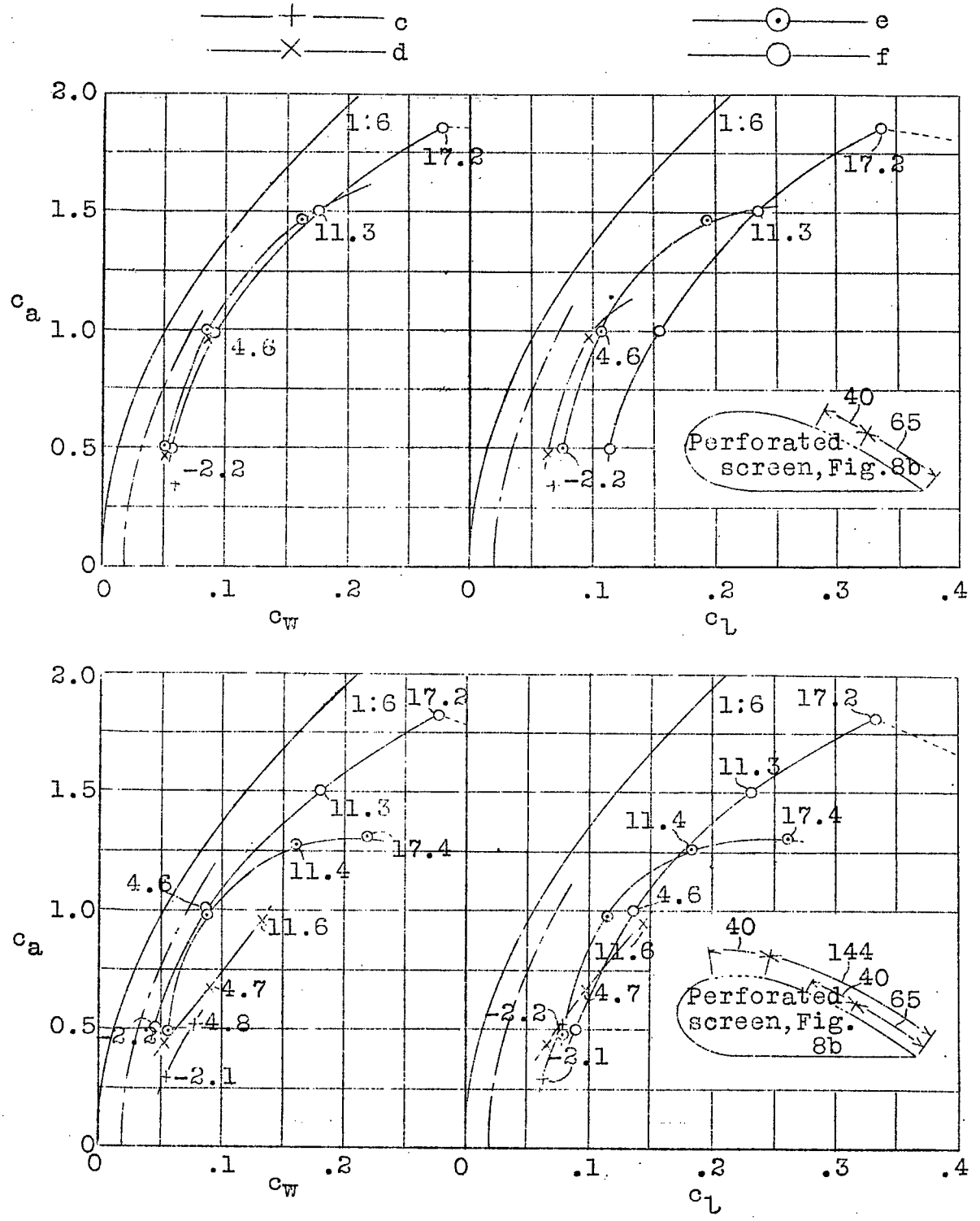

Figs.28 & 29 Polars of models in Section VIII with different suction arrangements.

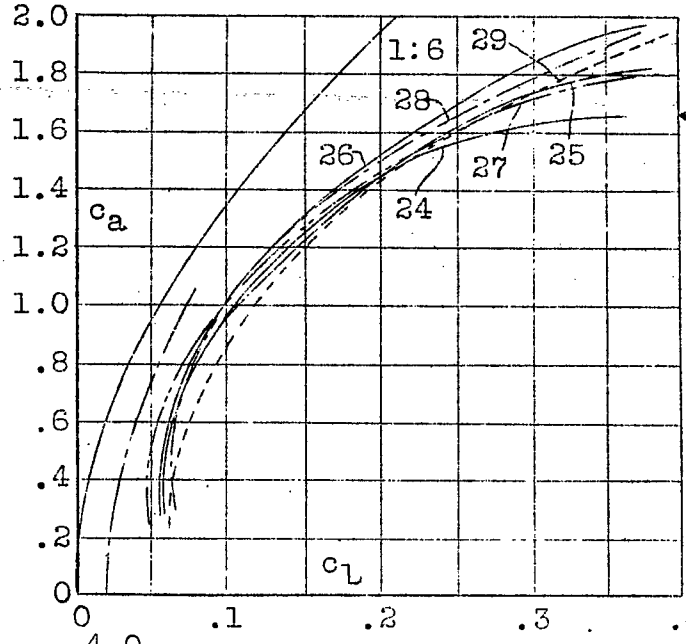

←Fig.30 Envelope polars for Figs.24 to Fig.29

Fig.31 Polars of central wing portion in Section VII . Figs.32 & 33.The lift element, produced by downward impulsion of suction air, is deducted. (See Section IV, footnote 3).